Beam Test of the SDC Double-sided Silicon Strip Detector

Y. Unno, F. Hinode, T. Akagi, T. Kohriki, N. Ujiie, *KEK*; Y. Iwata, T. Ohmoto, T. Ohsugi, T. Ohyama, *Hiroshima University*; T. Hatakenaka, N. Tamura, *Okayama University*; S. Kobayashi, A. Murakami, M. Tezuka, *Saga University*; R. Takashima, *Kyoto Education University*; T. Aso, H. Miyata, *Niigata University*; M. Daigo, *Wakayama Medical College*; M. Higuchi, *Tohoku-Gakuin University*; I. Kipnis, H. Spieler, *LBL*; J. DeWitt, D. Dorfan, A. Grillo, B. Hubbard, J. Rahn, W. Rowe, H. Sadrozinski, A. Seiden, E. Spencer, A. Webster, M. Wilder, *UC Santa Cruz*; M. Frautschi, J. Matthews, *University of New Mexico*; D. Kaplan, *University of Oklahoma*

Abstract

A beam test was executed to evaluate the behavior of the first prototype radiation-hard double-sided silicon microstrip sensor for the SDC silicon tracking system. Pions of 4 GeV/c in a test beamline at KEK illuminated three planes of detectors. The signals were amplified, shaped, and discriminated with TEKZ bipolar analog LSI's, and the on-off levels were sampled at 10MHz clock with CMOS digital LSI's, asynchronously with beam triggers. The detectors were rotated in null and 1.0 Tesla magnetic fields. The efficiencies were found to be 98~99%. The position resolutions were 12.5µm, where the multi-strip hit fraction was 30-40%. There was no essential difference in the performance of the p- and the n-sides. The multi-strip hit fraction showed a clear rotation and magnetic-field dependence. From the angles where the fractions were minimum in the 1T magnetic field, the Hall mobilities of the electrons and holes were obtained to be 1391±43 (electrons) and 325±30 (holes) cm^2/Vs.

I. INTRODUCTION

A beam test (T280) was executed at a test beam line at KEK to evaluate the performance of the first prototype of a radiation-hard design of the double-sided silicon microstrip sensor (DSSS). The sensor was designed for the barrel section of the silicon tracking system of the SDC detector [1] for physics at the SSC [2,3]. Due to the high interaction rate, one of the most stringent requirements for the sensors is radiation hardness. After a number of studies on radiation effects, we had worked out a radiation-hard design and produced the first prototype of the DSSS, the specifications of which are summarized in Table I. Axial strips were processed at the n-side and stereo strips (10 mrad stereo-angle) at the p-side, with a strip-pitch of 50 µm. It had AC coupling aluminum electrodes over the p- and n-strips sandwiching a SiO_2 insulator.

The SDC silicon tracking detector adopts a binary (on/off) readout scheme for its 6 million total readout channels. The shaping time constant of the front-end amplifier is expected to be about 20 ns to identify a hit to its own beam crossing, which occurs at a rate of 60 MHz. The silicon tracking system is imbedded in a solenoidal magnetic field of 2 Tesla for the momentum measurement. In the layout of the silicon tracking system, charged tracks hit the sensors at a maximum angle of 14° perpendicular to the axial strips and 60° along the strips.

TABLE I
SPECIFICATIONS OF THE RADIATION-HARD SDC DOUBLE-SIDED SILICON STRIP SENSOR (BARREL)

(1) Substrate	
Type	n-type Si
Resistivity	4~8 kΩ·cm
Thickness	300±10 µm
(2) Size	
Overall dimension[a]	60 mm×34.1 mm
Stereo-effective area	58.8 mm×31.4 mm
(3) Strip	
Pitch	50 µm
Stereo angle	10 mrad
Implant width	≥10, ≤12 µm
AC electrode width	<10 µm
Strip isolation of n-side	p$^+$ isolation line
(4) Capacitance	
AC coupling	≥20 pF/cm
p-side (body+interstrip)	≤1.2 pF/cm
n-side (body+interstrip)	≤1.4 pF/cm
(5) Bias resistor	
Polycrystalline silicon	250±50 kΩ

[a] Actual dimension is 60 µm narrower due to sawing

II. EXPERIMENT

Beamline Setup

The experiment was set up at the π2 test beamline of the 12-GeV proton synchrotron at KEK (Fig. 1). Five scintillation counters (S_1, S_2, S_3, F_1, and F_2) were set to make a trigger for the data-acquisition sequence. S_1, S_2, and S_3 had a scintillator of 2cm (width) × 2cm (height) × 5mm (thickness); S_2 and S_3 were placed close-by, but displaced to make an overlap of 1cm in the horizontal direction; two small counters (F_1 and F_2), each of which had dimensions of 5mm × 1cm × 3.2 mm, were placed in the shielding box for the detectors. The total coincidence of the five counters made a beam spot size of 5mm (in horizontal) × 1cm (in vertical) at the detectors. The timing was determined by S_3. Two

Cerenkov counters were used to differentiate pions and electrons (the fraction of electrons was ~6% of the total particles). The coordinate system was right-handed and +*z* in the beam-flow direction and +*y* in the vertically upward direction.

A dipole magnet (USHIWAKA) with an opening aperture of 82cm × 40cm × 70cm was placed in the down-stream of S_3 to provide a magnetic field (-*y* direction) having a maximum of 1.2 Tesla. An aluminum shielding box (60cm × 39cm × 65cm) was held inside the opening. Inside the shielding box, three planes of detectors were aligned in a mini-crate by butting the detectors to the optical mirror; the crate was held on a translation-rotation stage. The translation-rotation stage could move the crate in the *x*-direction, rotate in the ϕ angles around the *y*-axis, the θ angles around the (rotated) *x*-axis. Three planes of the detectors were separated by 8mm each to minimize the effect of multiple Coulomb scattering. For 4 GeV/c pions, the r.m.s. deviation of the middle plane out of the straight line through the 1st and 3rd planes was expected to be 0.3μm.

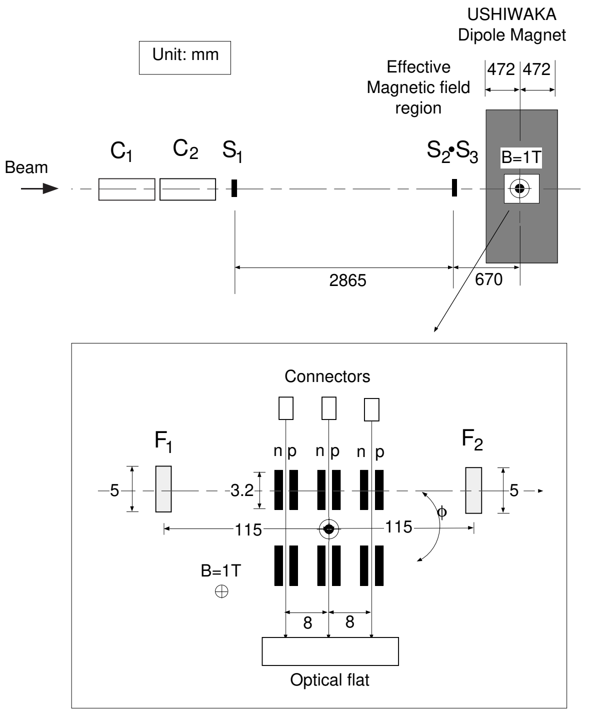

Fig. 1 Beamline setup of the T280 experiment used to evaluate the performance of the first prototype SDC double-sided silicon microstrip sensor.

Detectors

Three identical detectors were fabricated for the beamtest. One detector was made of one DSSS on a 12cm × 12 cm multi-layer PC board (Fig. 2). The basic building block of the readout front-end electronics was a pair of analog and digital LSI's. This scheme, an analog LSI being realized with bipolar technology and a digital LSI with CMOS technology, has been identified as being the best-suited for a fast, low-noise, and low-power consumption readout for the SDC detector [4]. In this detector board, there were two sets in each side of the board. The analog chips were TEKZ bipolar chips [5], having input/output of 64 channels and unipolar (Poisson) shaping with a time constant of ~30ns. The digital chips were CMOS SRAM buffer chips [6].

A block diagram of the sensor and the front-end electronics is shown in Fig. 3. A DSSS was reversely biased at 100V with a single DC power supply. The reference point which was connected to the front-end amplifier ground was made by dividing the potential with two 40MΩ resistors. This was to supply a symmetric potential difference to the AC coupling capacitors of the p- and n-sides of the DSSS. Signals were amplified, shaped, and discriminated (time over the threshold) to on-off levels with the analog chips. The discrimination threshold voltage (V_t) was controlled separately for the p-side and the n-sides (but not separately for the three detectors) and was set at 1.2fC. The on-off levels were transmitted to the digital chips, in which the levels were sampled and pipelined through the first level buffer of 64-bit depth at a 10 MHz clock continuously. With a trigger accept, which was asynchronous to the phase of the clock, a bunch of bits (3 in this experiment) was transferred to the level-2 buffer and then transferred to the output register for readout with the 10MHz clock.

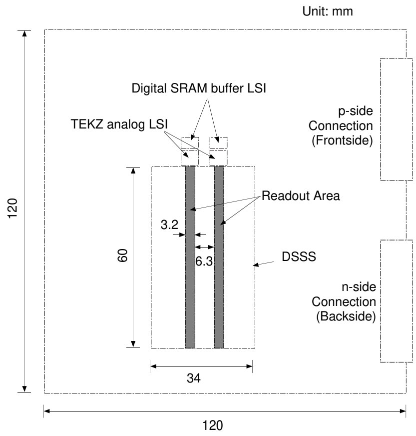

Fig. 2 Detector board layout used for the experiment. One DSSS was read out with two sets of 64 channel analog and digital LSI's per side. The two sets covered two separated 3.2mm wide areas of the DSSS.

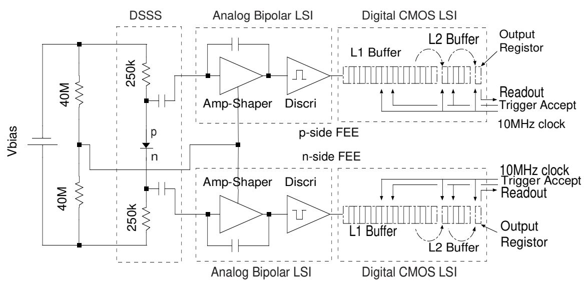

Fig. 3 Schematic block diagram of the DSSS and the front-end electronics. A 10 MHz clock was supplied continuously, regardless of trigger accepts.

Data Acquisition Flow

Fig. 4 shows the data-acquisition (DAQ) flow. The main feature of the DAQ was the use of the VME-UNIX system (UNIDAQ), which had been developed for experiments at the SSC [7]. A UNIX workstation (DEC station 5000/125) controlled the VME modules through the DEC Turbo-channel VME adapter in the workstation and the DEC PMABV-T6000-AA VME module in the VME crate. CAMAC modules were communicated via the VME.

A total coincidence of $S_1 \bullet S_2 \bullet S_3 \bullet F_1 \bullet F_2$ initiated the DAQ flow: a VME digital readout sequencer (DRS) module [8] to transfer the data from the front-end digital LSI's to a memory in the DRS and a CAMAC input register for the work station to process the data in the CAMAC and the VME modules. The DRS module received a 10 MHz clock, threshold voltages (V_t) and calibration signals to route to the detectors. The phase difference (in time) of a trigger and the clock was measured with a CAMAC TDC.

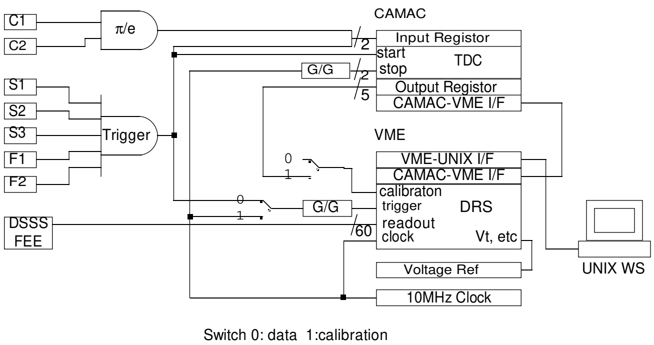

Fig. 4 Data-acquisition flow diagram. The main feature of the DAQ was the use of a VME-UNIX system (UNIDAQ).

Data Taking

Negatively charged pions of 4 GeV/c illuminated the center of the readout area of the connector-side chip set in an area of 5x10 mm^2 (The r.m.s size of the beam was ~1cm). The repetition cycle of the beam spill from the 12 GeV/c PS was 2sec out of an acceleration-extraction cycle of 4 sec. A typical number of triggers was ~1,000 per spill. The data-acquisition speed was ~200 events per spill.

The bias voltage was kept at 100 V: -50V to the p-side and +50V to the n-side relative to the amplifier ground. Data were collected in the null magnetic field (B=0T) for ϕ-rotations (Set#1) and for θ-rotations (Set#2,3,4), and in the 0.9937 Tesla magnetic field (B=1T) (Set#5). The threshold was kept at 1.2fC. At the normal incidence (Set#6), the thresholds were varied from 0 to 6fC at a step of 0.5fC. The conditions of the data set are summarized in Table II. The typical data quantity was 100k events per data point.

TABLE II.
SUMMARY OF DATA TAKEN FOR THE T280 BEAM TEST

Set	Variable	Fixed
#1	ϕ=0°, ±3°, ±6°, ±9°	θ=0°, V_t=1.2fC, B=0T
#2,3,4	θ=0°, ±18°, ±36°, ±54°	ϕ=0°, ±9°, V_t=1.2fC, B=0T
#5	ϕ=0°, ±1.5°, ±3°, ±4.5°, ±6°, ±7.5°, ±9°	θ=0°, V_t=1.2fC, B=1T
#6	V_t=0~6fC (0.5fC step)	ϕ=θ=0°, B=0T

III. RESULTS

Determination of Global Alignment

The alignment of the three detectors was obtained by using data set #1. Straight tracks were fitted to the clear events with unique hits in 6 measurement planes (p- and n-side × three detectors), assuming an incident angle of -ϕ. Six alignment parameters, x- and y- displacements and a rotation around z-axis of the 2nd and the 3rd detectors relative to the 1st detector $((\Delta x, \Delta y, \Psi)_2$ and $(\Delta x, \Delta y, \Psi)_3)$ were obtained by minimizing the distances of the fitted tracks to the axial and the stereo strips of the three planes at ϕ=0°. By fixing these six parameters, the relative z-displacements from the nominal 8mm of the 2nd and 3rd detectors (Δz_2 and Δz_3) were obtained, while again minimizing the distances using the angled tracks at $\phi \neq 0°$. These obtained 8 global alignment parameters are summarized in Table III.

TABLE III
GLOBAL ALIGNMENT PARAMETERS

Detector#	Δx (μm)	Δy (μm)	Δz (μm)	Ψ (mrad)
1	0.	0.	0.	0.
2	-350.8±0.4	-60±18	-506±8	-0.53±0.05
3	-134.9±0.6	-31±18	104±8	-0.25±0.08

In finding the hit position, a cluster was defined for the hit-strips adjacent to each other. For a cluster with n hit-strips, the hit position (x) was defined using the geometrical mean position of the n strips. Accordingly, the spatial-quantization unit was 25μm in a measurement plane (i.e. p- or n-side).

In the following analysis, three general criteria for the hits were imposed: Clock Timing Cut, Clear Event Cut, and Clear Track Cut.

(1) Clock Timing Cut: Since the clock phase was asynchronous to the trigger, the leading edge of the clock occurred continuously relative to the particle passage. Since the pulse peaking time was ~30 ns, only those events were accepted in a 40ns interval where the signal peaks were estimated to fall at about the first 1/3 point.

(2) Clear Event Cut: Because there were dead channels and edges of the readout area, only those events were accepted

which did not have a hit or an interpolated hit position (defined below) adjacent to the dead channels or to the edge channels.

(3) Clear Track Cut: A straight track was calculated by connecting the cross-point of the p- and n-side hits of the 1st detector and that of the 3rd detector. Only those tracks were accepted to have an angular deviation within ±1° from the nominal values.

In a magnetic field of 1T, incident charged particles were deflected before arriving at the silicon detectors. This deflection was obtained to be -2.09±0.002° in situ. The ϕ angles of the 1T magnetic field were corrected by this amount in the following figures.

Efficiency

The efficiencies of the p- and the n-side of the 2nd detector were evaluated by counting whether there was a hit in the side. A hit was searched within ±110μm from the interpolated position of the calculated tracks. No obvious inefficiency was observed in the 64 channels of the p- and the n-sides in the three detectors, other than dead channels.

The efficiencies of the p- and the n-side of the 2nd detector are plotted as a function of ϕ angles (Fig. 5). Fig. 5(a) is for B=0T and Fig. 5(b) for B=1T. There is an undulation in the data which might have been caused by the loss of signals (see in the discussion in the multi-strip hit fraction); in general, however, the efficiencies were as high as 98~99%, regardless of the p- and the n-sides and existence of the magnetic field.

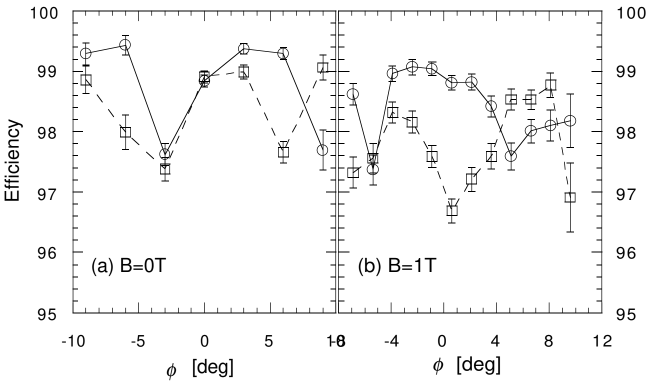

Fig. 5 Efficiency of the p-side (circle/solid line) and n-side (square/dashed line) of the 1st prototype SDC double-sided silicon microstrip sensor: (a) no magnetic field, (b) a 1T magnetic field.

Position Resolution

The spatial position resolutions of the p- and n-sides of the 2nd detector were estimated using the residuals of the hits in the p- or n-side to the interpolated position of the calculated track using the hits in the 1st and the 3rd detectors, effectively defined by $\delta=(x_1+x_3)/2-x_2$. Here, x is the distance normal to the strip. A typical residual distribution is given in Fig. 6, which shows a quantization effect. This quantization of unit of 12.5μm was caused by the quantization of measurements in a plane having a unit of 25μm. In order to obtain the resolution, a Gaussian was fitted to the re-binned distribution with a bin size of 12.5μm and the center of the bin at the peak position of the quantization to dismiss the effect.

The formula used to give a single-side resolution was $\sigma_S=0.895\times\sigma_\delta$, instead of $\sigma_S=\sqrt{2/3}\,\sigma_\delta$, by taking into account the 10mrad stereo angle and the use of two measurement points in defining x_1 and x_3. The position resolutions varied as a function of the ϕ angles and were 12.5μm, where the multi-strip fraction was 30~40% (Fig. 7).

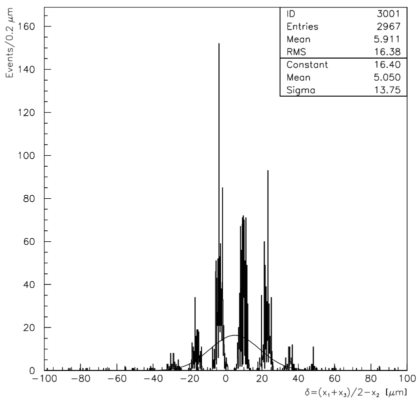

Fig. 6 Typical residual distribution: p-side, ϕ=+8.1°, B=1T.

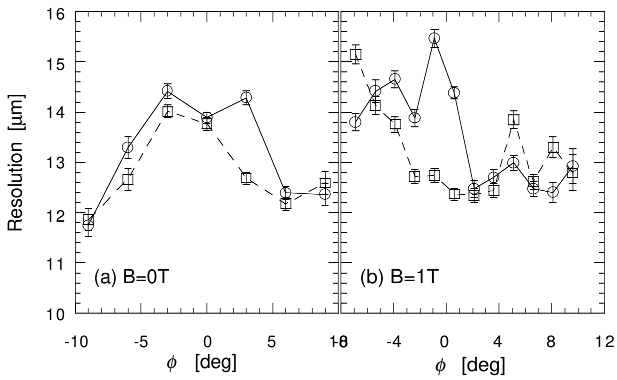

Fig. 7 Position resolutions of the p-side (circles/solid line) and n-side (squares/dashed line) as a function of the ϕ angles: (a) B=0T, (b) B=1T.

Multi-strip Hit Fraction

The swath of generated electron-hole pairs along their passages of charged particles in 300μm silicon spreads over more than single strip, depending on the incident angles or the existence of a magnetic field. A signal simulation shows that the position resolution will be improved by more than the pitch/$\sqrt{12}$ due to the separation of single-strip-hit and double-strip-hit regions; there is an angle in which electrons and holes are collected over equal sized spans in the p- and n-sides [9]. The Hall mobilities of the electrons and holes must be known to determine this tilt angle.

The multiple-strip hit fraction distributions show clear angular and magnetic field dependencies (Fig. 8). The n-side fraction was higher than that of the p-side, possibly due to the larger diffusion of electrons and greater electronic noise in the n-side. There is a clear correlation between the fraction and position resolution; the best position resolution was obtained when the fraction was 30-40%. There was, however, a slight anti-correlation between the fraction and efficiency; the threshold of 1.2fC might have been a bit too high.

The ϕ-angles where the fractions are minimum corresponds to the Hall angles of the carriers. The curves in Fig. 8 were fitted lines to a hyperbolic function, $y=c\sqrt{1+(x-a)^2/b}$. After calibrating the ϕ-angle readout-offsets using the B=0T data, the Hall angles (θ_H) were obtained to be -1.85±0.17° (holes: p-side) and +7.87±0.24° (electrons: n-side), which correspond to the Hall mobilities (μ_H) of 325±30 (holes) and 1391±43 cm^2/Vs (electrons) using the relation $\tan\theta_H=10^{-8}\mu_H B$. The dopant concentration of the silicon was estimated to be $(1.02\pm0.15)\times10^{12}$ cm^{-3} from a measurement of the depletion voltage.

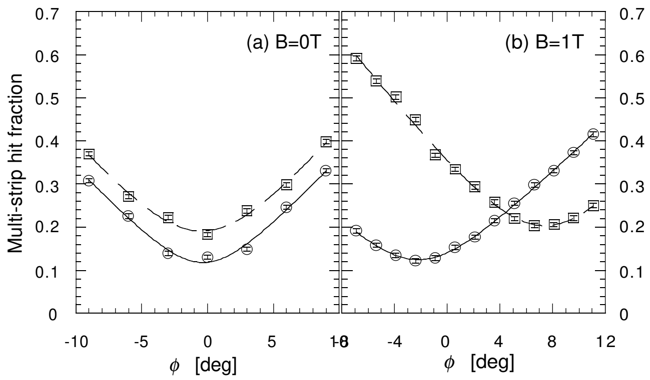

Fig. 8 Multi-strip hit fraction as a function of the ϕ-angles: (a) B=0T, (b) B=1T; p-side (circle/solid line), n-side (square/dashed line). The curves are fitted lines to a hyperbolic function, $y=c\sqrt{1+(x-a)^2/b}$.

Signal-to-Noise Ratio

Using data set #6 (threshold variation) the efficiencies of the 2nd detector were obtained as a function of the threshold voltage. By fitting an error function to the variation, the gain of the amplifier was determined by regarding the 50% point as being the most probable energy deposition of 4fC in 300µm silicon. The gain was slightly more than 100 mV/fC for both the p- and n-sides. The electronic noise was determined from pulsar calibration runs, and was found to be 22 and 25 mV for the p- and n-sides, respectively. The signal/noise ratios were 18 and 16, respectively.

IV. CONCLUSION

The first prototype of a radiation-hard double-sided silicon microstrip sensor for the SDC experiment at the SSC was successfully beam tested using 4 GeV/c pions at KEK. The front-end readout scheme used in the test was conceptually the same as the proposed scheme: bipolar analog LSI's and CMOS digital LSI's; binary (on/off) readout; and continuous clocking. TEKZ analog LSI's (τ~30ns) and CMOS SRAM digital LSI's were used for the readout electronics, and the digital chips were clocked at 10MHz asynchronously with the beam triggers. The front-end electronics were interfaced with a digital readout sequencer (DRS) to a VME-UNIX data-acquisition system (UNIDAQ). Data were taken in the null and 1T magnetic fields and by rotating the three planes of the detectors in ϕ and θ directions.

The efficiencies and position resolutions of the p- and n-sides of the middle detector were evaluated as a function of the ϕ-rotation angles by using the 1st and 3rd detectors as the defining anchors. The efficiencies were found to be 98~99%, depending on the ϕ-angle and the existence of a magnetic field. The position resolutions were as good as 12.5µm, where the multi-strip hit fraction was 30-40%. There was no essential difference in the performance of the p- and the n-sides. The multi-strip hit fraction showed a clear rotation and a magnetic-field dependence. From the angles where the fractions were minimum in the 1T magnetic field, the Hall mobilities of the electrons and holes were obtained to be 1391±43 (electrons) and 325±30 (holes) cm^2/Vs, respectively.

V. ACKNOWLEDGMENTS

This work was supported in part by the Japan-US cooperation in the field of high-energy physics, by a Grant-in-Aid for Joint Research in the International Scientific Research Program of Ministry of Education, Science and Culture, of Japan, and by the US Department of Energy. The authors would like to thank the support of the staff of the PS section of KEK.

VI. REFERENCES

[1] T. Ohsugi et al., Double-sided Microstrip Sensor for the Barrel of the SDC Silicon Tracker, in the Int. Symp. Dev. Appl. of Semiconductor Tracking Detectors (Hiroshima STD Symposium), May 22-24, 1993, Hiroshima, the proceedings to be published in Nucl. Instr. Meth. Sec. A; T. Ohsugi, et al., Prototype Double Sided Silicon Sensor (DSSS) for SDC Detector, IEEE Nucl. Scie. Symp. at Orlando, Oct. 25-30, 1992. The microstrip sensors were fabricated by Hamamatsu Photonics, Co. Ltd, Hamamatsu 430, Japan

[2] A. Weinsten et al., Silicon Tracking Conceptual Design Report, SCIPP 92/04, University of California, March 1992

[3] Y. Unno, The SDC Silicon Tracking System, in the Hiroshima STD Symposium

[4] Ref. 2; H. Spieler and D. Dorfan in the Hiroshima STD Symposium.

[5] E. Barberis, et al., IEEE Trans. Nucl. Scie. 40(1993)740

[6] J. DeWitt, Nucl. Instr. Meth. A288(1990)209

[7] A. Fry and M. Nomachi, UNIDAQ: a portable data-acquisition system for SSC detector R&D, 8th Real-time Computer Applications in Nuclear, Particle, and Plasma Physics (RT93), June 8-11, 1993, Vancouver, Canada

[8] B. Hubbard et al., A Digital Readout Sequencer (DRS), SCIPP 93/43, Univ. of California, Santa Cruz

[9] J. Leslie, A. Seiden, Y. Unno, SCIPP 92/20, Univ. of California, Santa Cruz; IEEE Trans. Nucl. Scie., 40(1993)557